AD-A178 557 PHASE SPACE METHODS AND PATH INTEGRATION: A MICROSCOPIC APPROACH TO DIREC..(U) CATHOLIC UNIV OF AMERICA WASHINGTON D C DEPT OF CIVIL ENGINEE.. L FISHMAN 1/1

UNCLASSIFIED 05 FEB 87 ARO-20910.6-MA DAAG29-85-K-0002 F/G 20/1 NL

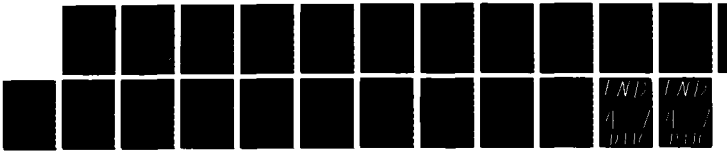

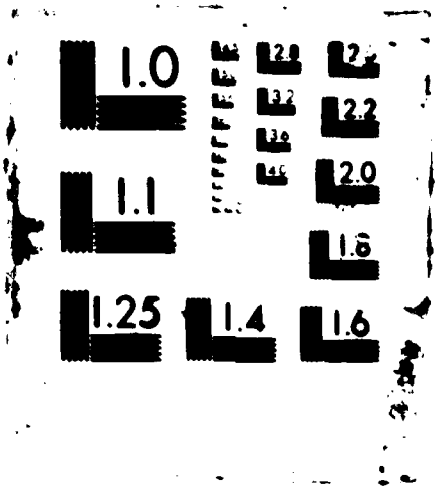
1.0
1.1
1.25
1.4
1.6
2.2
2.0
1.8

PHASE SPACE METHODS AND PATH INTEGRATION:

A MICROSCOPIC APPROACH TO DIRECT AND INVERSE WAVE PROPAGATION

Final Report

Louis Fishman

February 6, 1987

U.S. ARMY RESEARCH OFFICE

DAAG29-85-K-0002

The Catholic University of America
Washington, D.C. 20064

APPROVED FOR PUBLIC RELEASE
DISTRIBUTION UNLIMITED

UNCLASSIFIED
SECURITY CLASSIFICATION OF THIS PAGE

REPORT DOCUMENTATION PAGE

1a. REPORT SECURITY CLASSIFICATION Unclassified	1b. RESTRICTIVE MARKINGS
2a. SECURITY CLASSIFICATION AUTHORITY	3. DISTRIBUTION/AVAILABILITY OF REPORT Approved for public release; distribution unlimited.
2b. DECLASSIFICATION/DOWNGRADING SCHEDULE	
4. PERFORMING ORGANIZATION REPORT NUMBER(S)	5. MONITORING ORGANIZATION REPORT NUMBER(S) ARO 20910.6-MA
6a. NAME OF PERFORMING ORGANIZATION The Catholic University of America 6b. OFFICE SYMBOL (If applicable)	7a. NAME OF MONITORING ORGANIZATION U. S. Army Research Office
6c. ADDRESS (City, State, and ZIP Code) Washington, DC 20064	7b. ADDRESS (City, State, and ZIP Code) P. O. Box 12211 Research Triangle Park, NC 27709-2211
8a. NAME OF FUNDING/SPONSORING ORGANIZATION U. S. Army Research Office 8b. OFFICE SYMBOL (If applicable)	9. PROCUREMENT INSTRUMENT IDENTIFICATION NUMBER DAAG29-85-K-0002
8c. ADDRESS (City, State, and ZIP Code) P. O. Box 12211 Research Triangle Park, NC 27709-2211	10. SOURCE OF FUNDING NUMBERS PROGRAM ELEMENT NO. / PROJECT NO / TASK NO. / WORK UNIT ACCESSION NO

11. TITLE (Include Security Classification)
PHASE SPACE METHODS AND PATH INTEGRATION:
A Microscopic Approach to Direct and Inverse Wave Propagation

12. PERSONAL AUTHOR(S)
Louis Fishman

13a. TYPE OF REPORT	13b. TIME COVERED	14. DATE OF REPORT (Year, Month, Day)	15. PAGE COUNT
Final	FROM 11/84 TO 11/86	February 5, 1987	19

16. SUPPLEMENTARY NOTATION
The view, opinions and/or findings contained in this report are those of the author(s) and should not be construed as an official Department of the Army position, policy, or decision, unless so designated by other documentation.

17. COSATI CODES		
FIELD	GROUP	SUB-GROUP

18. SUBJECT TERMS (Continue on reverse if necessary and identify by block number)
Helmholtz equation, factorization, path integral, pseudo-differential operator, Fourier integral operator, marching algorithm, invariant imbedding, Monte Carlo, inverse methods

19. ABSTRACT (Continue on reverse if necessary and identify by block number)

This project focuses on the development of new, multidimensional algorithms for direct acoustic propagation and generalized acoustic tomography at the level of the scalar Helmholtz equation. The general aim is the continued detailed development of the ideas originally outlined several years ago. Phase space, or "microscopic," methods and path (functional) integral representations provide the appropriate framework to extend homogeneous Fourier methods to inhomogeneous environments. The path integrals furnish the principal representation of the Helmholtz propagator and, subsequently, through direct computation, the basis for the direct numerical algorithms. There are two complementary approaches to the analysis and computation of the n-dimensional Helmholtz propagator. The first is essentially a factorization/parabolic-based (one-way) phase space path integration/invariant imbedding approach. This results in a marching algorithm for one-way wave propoagation, a nonperturbative incorporation of backscatter effects which generalizes Kennett's algorithm in reflection seismology for two-way wave propagation,

20. DISTRIBUTION/AVAILABILITY OF ABSTRACT ☐ UNCLASSIFIED/UNLIMITED ☐ SAME AS RPT. ☐ DTIC USERS	21. ABSTRACT SECURITY CLASSIFICATION Unclassified
22a. NAME OF RESPONSIBLE INDIVIDUAL	22b. TELEPHONE (Include Area Code) / 22c. OFFICE SYMBOL

DD FORM 1473, 84 MAR 83 APR edition may be used until exhausted. All other editions are obsolete

SECURITY CLASSIFICATION OF THIS PAGE
UNCLASSIFIED

and the basis for the formulation and solution of corresponding arbitrary-dimensional nonlinear inverse problems. The numerical algorithms based on these modern, "microscopic" methods directly compute pseudo-differential and Fourier integral operators, incorporate phase space filtering, and are ideally suited for computers which provide either a vector or a parallel pipe type of operation. Extensive testing has, so far, been very promising. While the first approach starts from a transversely inhomogeneous formulation and, subsequently, builds in backscatter effects, the second approach constructs elliptic-based (two-way) path integral representations of the propagator for general range-dependent environments from the outset. A particular approximate path integral construction (Feynman/Garrod) results in a true path functional, suggesting the underlying stochastic foundations of the Helmholtz equation. It appears to be a viable computational approximation for a useful range of propagation experiments and can be numerically evaluated by standard Monte Carlo (statistical) methods. A more detailed examination and approximate construction of the underlying stochastic process would provide for both more accurate and widely applicable path integral representations and direct numerical simulation techniques.

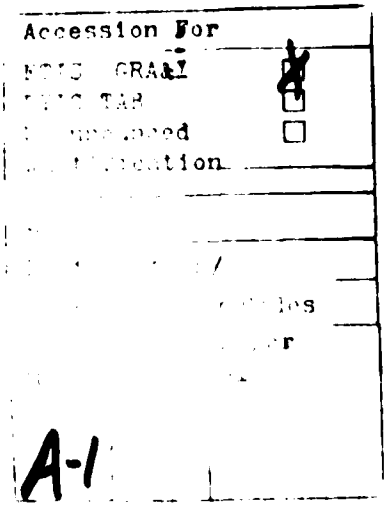

PHASE SPACE METHODS AND PATH INTEGRATION:

A MICROSCOPIC APPROACH TO DIRECT AND INVERSE WAVE PROPAGATION

Louis Fishman
Department of Civil Engineering
The Catholic University of America
Washington, D.C. 20064 USA

ABSTRACT. This project focuses on the development of new, multidimensional algorithms for direct acoustic propagation and generalized acoustic tomography at the level of the scalar Helmholtz equation. The general aim is the continued detailed development of the ideas originally outlined several years ago. Phase space, or "microscopic," methods and path (functional) integral representations provide the appropriate framework to extend homogeneous Fourier methods to inhomogeneous environments. The path integrals furnish the principal representation of the Helmholtz propagator and, subsequently, through direct computation, the basis for the direct numerical algorithms. There are two complementary approaches to the analysis and computation of the n-dimensional Helmholtz propagator. The first is essentially a factorization/parabolic-based (one-way) phase space path integration/invariant imbedding approach. This results in a marching algorithm which generalizes the Tappert/Hardin split-step FFT algorithm for one-way wave propagation, a nonperturbative incorporation of backscatter effects which generalizes Kennett's algorithm in reflection seismology for two-way wave propagation, and the basis for the formulation and solution of corresponding arbitrary-dimensional nonlinear inverse problems. The numerical algorithms based on these modern, "microscopic" methods directly compute pseudo-differential and Fourier integral operators, incorporate phase space filtering, and are ideally suited for computers which provide either a vector or a parallel pipe type of operation. Extensive testing has, so far, been very promising. While the first approach starts from a transversely inhomogeneous formulation and, subsequently, builds in backscatter effects, the second approach constructs elliptic-based (two-way) path integral representations of the propagator for general range-dependent environments from the outset. A particular approximate path integral construction (Feynman/Garrod) results in a true path functional, suggesting the underlying stochastic foundations of the Helmholtz equation. It appears to be a viable computational approximation for a useful range of propagation experiments and can be numerically evaluated by standard Monte Carlo (statistical) methods. A more detailed examination and approximate construction of the underlying stochastic process would provide for both more accurate and widely applicable path integral representations and direct numerical simulation techniques.

I. INTRODUCTION. Direct wave propagation modeling plays a significant role in such fields as underwater communication, radio transmission through the atmosphere, laser propagation, and earthquake prediction. Likewise, the corresponding inverse problems are at the heart of such areas as submarine detection, CAT scan technology, soft-tissue diffraction tomography, the mapping of the interior earth, and oil

exploration. In all of these and many other examples, relatively fast and accurate numerical algorithms are necessary.

The analysis and fast, accurate numerical computation of the wave equations of classical physics are often quite difficult for rapidly changing, multidimensional environments extending over many wavelengths. For the most part, classical, "macroscopic" methods have resulted in direct wave field approximations (perturbation theory, ray-theory asymptotics, modal analysis, hybrid ray-mode methods), derivations of approximate wave equations (scaling analysis, field splitting techniques, formal operator expansions), and discrete numerical approximations (finite differences, finite elements, spectral methods). In the last several decades, however, mathematicians studying linear partial differential equations have developed, in the language of physicists, a sophisticated, "microscopic" phase space analysis. In conjunction with the global functional integral techniques pioneered by Wiener (Brownian motion) and Feynman (quantum mechanics), and so successfully applied today in quantum field theory and statistical physics, the n-dimensional classical physics propagators can be both represented explicitly and computed directly. The phase space, or "microscopic," methods and path (functional) integral representations provide the appropriate framework to extend homogeneous Fourier methods to inhomogeneous environments, in addition to suggesting the basis for the formulation and solution of corresponding arbitrary-dimensional nonlinear inverse problems. Moreover, it is in phase space, rather than in configuration space, that, from a mathematical perspective, the interesting geometry takes place.

II. PHASE SPACE AND PATH INTEGRAL CONSTRUCTIONS. For the n-dimensional scalar Helmholtz equation, there are two complementary approaches to this analysis and computation, as illustrated in Figure 1. The first is essentially a factorization/path integration/invariant imbedding approach. For transversely inhomogeneous environments, implying medium homogeneity with respect to a single distinguished direction, the n-dimensional Helmholtz equation can be exactly factored into separate, physical forward and backward, one-way wave equations, following from spectral analysis [1-5]. The forward evolution (one-way) equation

$$(i/\bar{k})\partial_x \phi^+(x,\underline{x}_t) + (K^2(\underline{x}_t) + (1/\bar{k}^2)\nabla_t^2)^{1/2}\,\phi^+(x,\underline{x}_t) = 0\ , \qquad (1)$$

where $K(x)$ is the refractive index field and $\bar{k}$ is a reference wave number, is the formally exact wave equation for propagation in a transversely inhomogeneous half-space supplemented with appropriate outgoing wave radiation and initial-value conditions. While functions of a finite set of commuting self-adjoint operators can be defined through spectral theory, functions of noncommuting operators are represented by pseudo-differential operators [2,5]. The formal wave equation (1) is now written explicitly as a Weyl pseudo-differential equation in the form

$$(i/\bar{k})\partial_x \phi^+(x,\underline{x}_t) + (\bar{k}/2\pi)^{n-1} \int_{R^{2n-2}} d\underline{x}_t' d\underline{p}_t$$

$$\cdot\, a_B(\underline{p}_t,(\underline{x}_t + \underline{x}_t')/2)\, \exp(i\bar{k}\underline{p}_t\cdot(\underline{x}_t - \underline{x}_t'))\,\phi^+(x,\underline{x}_t') = 0. \qquad (2)$$

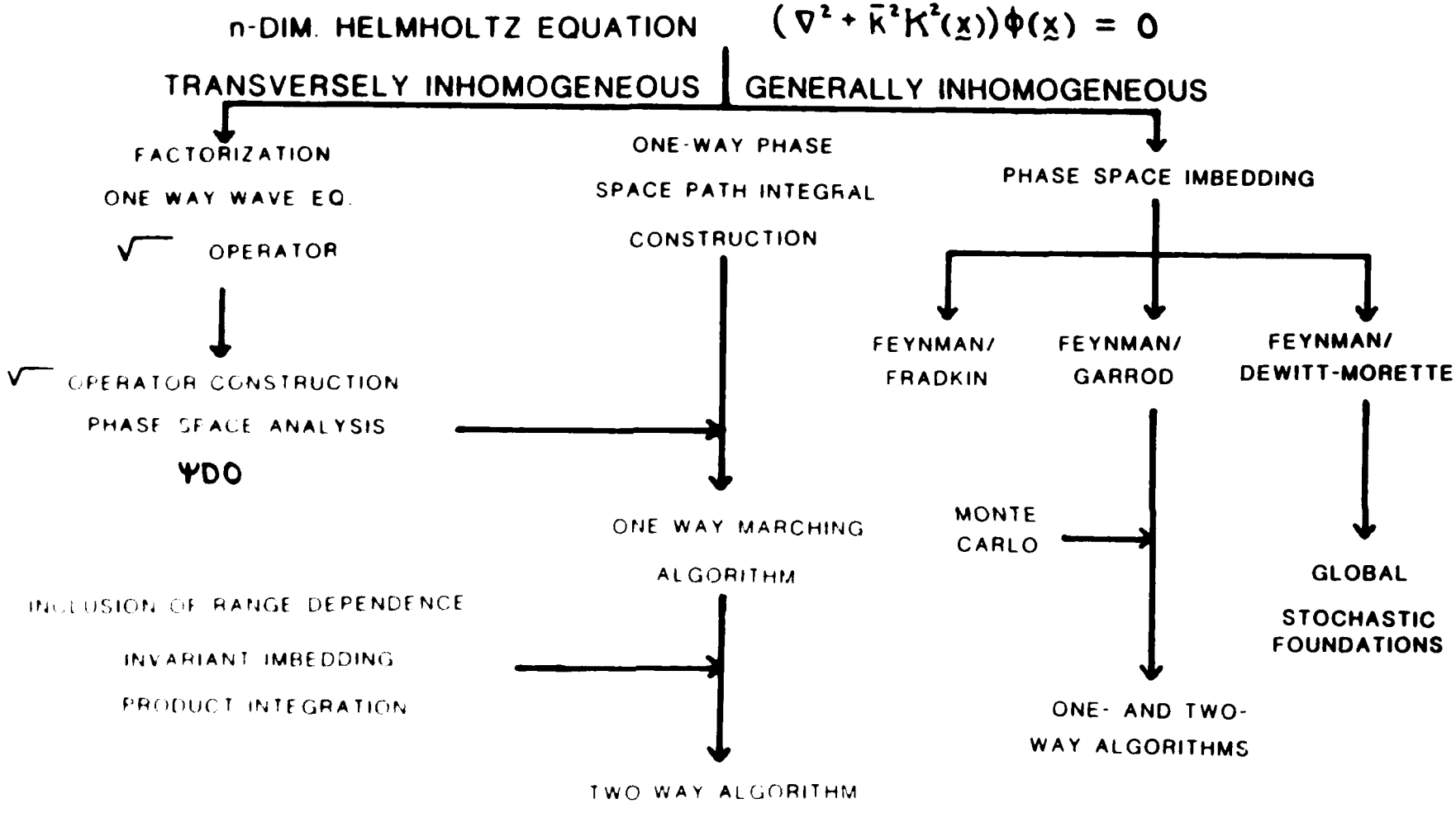

[illegible] elementary approaches to the analysis and computation of the n-dimensional scalar [illegible] equation

In Eq.(2), the symbol $\Omega_B(\underline{p},\underline{q})$ associated with the square root Helmholtz operator $B = (K^2(\underline{q}) + (1/\bar{k}^2)\nabla_{\underline{q}}^2)^{1/2}$ satisfies the Weyl composition equation

$$\Omega_B 2(\underline{p},\underline{q}) = K^2(\underline{q}) - \underline{p}^2 = (\bar{k}/\pi)^{2n-2} \int_{R^{4n-4}} d\underline{t}d\underline{x}d\underline{y}d\underline{z}\ \Omega_B(\underline{t}+\underline{p},\ \underline{x}+\underline{q})$$

$$\cdot \Omega_B(\underline{y}+\underline{p},\ \underline{z}+\underline{q})\ \exp(2i\bar{k}(\underline{x}\cdot\underline{y} - \underline{t}\cdot\underline{z})) \qquad (3)$$

with $\Omega_B 2(\underline{p},\underline{q})$ the symbol associated with the square of B, $B^2 = (K^2(\underline{q}) + (1/\bar{k}^2)\nabla_{\underline{q}}^2)$ [2,3,5]. The generalized Fourier construction procedure for the square root Helmholtz operator can be summarized pictorially by the following correspondence diagram

$$\begin{array}{ccc} B^2 & \Longleftrightarrow & \Omega_B 2 \\ \Uparrow & & \Updownarrow \\ B & \Longleftrightarrow & \Omega_B \end{array}$$

where the arrows symbolize the one- and two-way mappings between the appropriate quantities.

Exact solutions of the Weyl composition equation (3) can be constructed in several cases [6]. For example, the symbol $\Omega_B(p,q)$ for the two-dimensional (n = 2) quadratic medium, $K^2(q) = K_0^2 + w^2q^2$, is given by [6]

$$\Omega_B(p,q) = -(\exp(i\pi/4)\varepsilon^{1/2}/\pi^{1/2}) \int_0^\infty dt\ \exp(i(Yt + X\tanh t))$$

$$\cdot t^{-1/2}\ (iY\operatorname{sech} t + iX\operatorname{sech}^3 t - (\operatorname{sech} t)(\tanh t)) \qquad (4)$$

with $X = (1/\varepsilon)(w^2q^2 - p^2)$, $Y = K_0^2/\varepsilon$, and $\varepsilon = w/\bar{k}$. Consistent with taking the square root of the indefinite Helmholtz operator, the corresponding symbols, generally, have both real and imaginary parts characterized by oscillatory behavior [4,6], as illustrated in Figure 2. Nonuniform and uniform perturbation solutions corresponding to definite physical limits (frequency, propagation angle, field strength, field gradient) recover several known approximate wave theories (ordinary parabolic, range-refraction parabolic, Grandvuillemin-extended parabolic, half-space Born, Thomson-Chapman, rational linear) and systematically lead to several new full-wave, wide-angle approximations [2-4,6].

The exact pseudo-differential evolution equation (2) and, in general, the wide-angle extended parabolic approximate equations derived from the analysis of the composition equation [2-4,6] are singular integro-differential wave equations. Solution representations for such pseudo-differential equations can be directly expressed in terms of infinite-dimensional functional, or path, integrals [7,8], following from the Markov property of the propagator. In an operator notation, then,

$$\exp(i\bar{k}\hat{B}x) = \lim_{N\to\infty} \prod_{j=1}^{N} \exp(i\bar{k}\hat{B}\Delta x_j) \tag{5}$$

where $\Delta x_j = x/N$, symbolically representing the propagator in terms of the infinitesimal propagator. As the operator symbol is not simply quadratic in $\underline{p}$, the configuration space Feynman path integral formulation is not appropriate, necessitating the more general phase space construction [4,7]. This results in a parabolic-based (one-way) Hamiltonian phase space path integral representation of the propagator in the form [3,7]

$$G^{+}(x,\underline{x}_t|0,\underline{x}_t') = \lim_{N\to\infty} \int_{R^{(n-1)(2N-1)}} \prod_{j=1}^{N-1} d\underline{x}_{jt} \prod_{j=1}^{N} (\bar{k}/2\pi)^{n-1} d\underline{p}_{jt}$$

$$\cdot \exp\left(i\bar{k} \sum_{j=1}^{N} (\underline{p}_{jt}\cdot(\underline{x}_{jt} - \underline{x}_{j-1t}) + (x/N)\, H(\underline{p}_{jt},\underline{x}_{jt},\underline{x}_{j-1t}))\right) \tag{6}$$

where

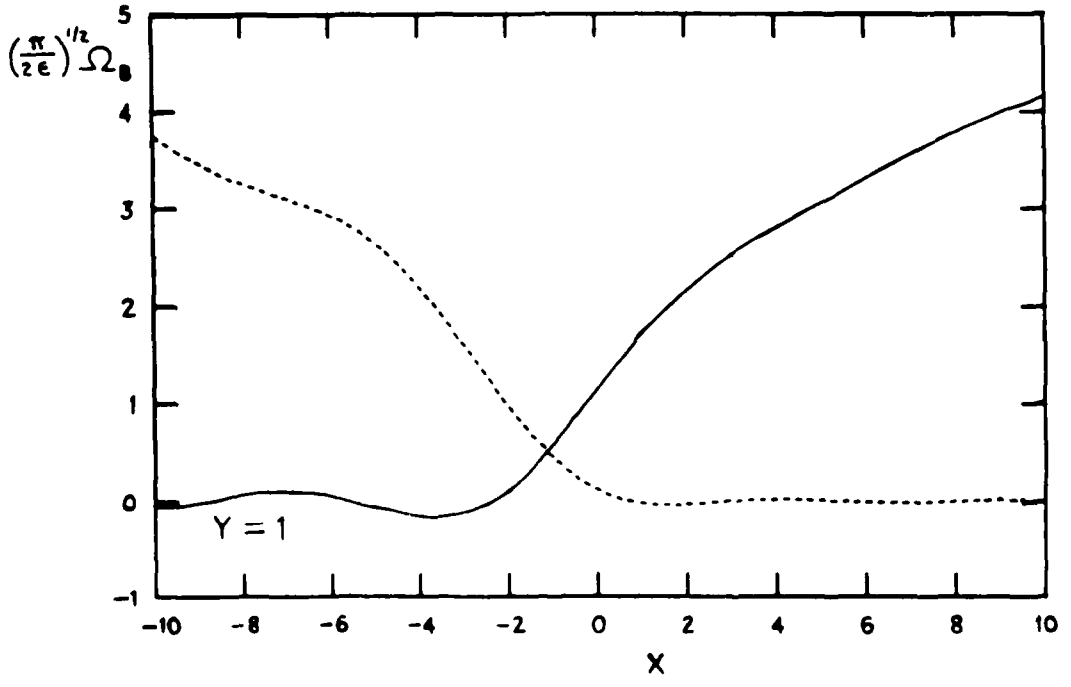

Fig. 2. The real (——) and imaginary (----) parts of the n = 2 quadratic medium symbol as a function of X for Y = 1.

$$H(\underline{p},\underline{q}'',\underline{q}') = (k/2\pi)^{n-1} \int_{R^{2n-2}} d\underline{s}d\underline{t}\, F(\underline{q}'-\underline{q}'',\underline{s})$$

$$\cdot h_B(\underline{p},((\underline{q}''+\underline{q}')/2) - \underline{t}) \exp(ik\underline{s}\cdot\underline{t}). \qquad (7)$$

In Eq.(7), $F(\underline{u},\underline{v})$ and $h_B(\underline{p},\underline{q})$ are related to the operator symbol $\Omega_B(\underline{p},\underline{q})$ by

$$\hat{\Omega}_B(\underline{u},\underline{v}) = F(\underline{u},\underline{v})\, \hat{h}_B(\underline{u},\underline{v}) \qquad (8)$$

where $\hat{\Omega}_B$ and $\hat{h}_B$ are the corresponding Fourier transforms [2,3,7].

The nonuniqueness of the lattice-approximation path integral representation is readily understood in terms of different discretizations, or quadratures, of the symbolic functional integral and corresponds to the representation of a given (fixed) operator by different operator-ordering, or pseudo-differential operator, schemes [2,3,7,8]. More fundamentally, in analogy with the Schrödinger equation for particle motion on a Riemannian space and the thermodynamic (Fokker-Planck) equation for particle diffusion, the algorithmic Helmholtz path integral construction reflects the stochastic nature of the integration [4,9]. Further, both the macroscopic and microscopic (infinitesimal) half-space propagators can be formally expressed as Fourier integral operators with complex phase [4]. The phase space path integral, thus, represents the macroscopic Fourier integral operator in terms of the N-fold application of the microscopic, or infinitesimal, Fourier integral operator in a manner which can be related to the global geometrical-optics construction of the macroscopic operator [4,5].

The path integral formulation interprets the wave theory in terms of an infinitesimal propagator summed over all phase space paths. For the Helmholtz theory, the exact infinitesimal propagator is not, in general, given by the locally homogeneous medium propagator, as in the ordinary parabolic (Schrödinger) propagator construction [8]. The approximate extended parabolic wave theories then correspond to approximate *infinitesimal propagators* summed over the complete phase space. In retaining the "sum over all paths," diffraction, or full-wave, effects are incorporated.

For weakly range-dependent environments, range variability can be, at first, accommodated at the level of range updating, as in the case of the parabolic path integral [1,8]. For reflection/transmission from a planar interface separating two (different) transversely inhomogeneous acoustic half-spaces, the concept of reflection and transmission amplitudes generalizes to reflection (r) and transmission (t) operators. The reflection and transmission operators, which, when applied to the incident wave field at the interface, produce the initial values of the reflected and transmitted wave fields, are defined within the Weyl pseudo-differential operator framework and are explicitly determined by enforcing the well-known interface continuity conditions. The main result [10] is a composition equation of the form

$$\Omega_{BL}(\underline{p},\underline{q}) - \Omega_{BR}(\underline{p},\underline{q}) = (k/\pi)^{2n-2} \int_{R^{4n-4}} d\underline{t}d\underline{x}d\underline{y}d\underline{z}\, (\Omega_{BL}(\underline{t}+\underline{p},\ \underline{x}+\underline{q}) +$$

$$\Omega_{BR}(\underline{t}+\underline{p},\ \underline{x}+\underline{q})\ \Omega_r(\underline{y}+\underline{p},\ \underline{z}+\underline{q})\ \exp(2i\bar{k}(\underline{x}\cdot\underline{y} - \underline{t}\cdot\underline{z})) \qquad (9)$$

for the reflection operator symbol $\Omega_r(\underline{p},\underline{q})$ and an analogous equation for the transmission operator symbol $\Omega_t(\underline{p},\underline{q})$. The inclusion of a planar transition region of arbitrary length and inhomogeneity can be accomplished by factorization methods in conjunction with invariant imbedding [4,11]. Invariant imbedding constructs the initial-value system for the reflection and transmission operators associated with the transition region, transforming the Helmholtz boundary-value problem into an initial-value problem. A discretized formulation [11] provides the extension of Kennett's method [4,11] in reflection seismology. The resultant forward and backward wave fields propagating in the transversely inhomogeneous half-spaces are represented by the one-way path integrals, while, within the transition region, a formal path integral representation of the propagator can be expressed as a product integral [8]. This takes the form [4]

$$G = \int_a^{\cup x} \exp(i\bar{k}\underline{\underline{H}}(s)ds) = \lim_{N\to\infty} \prod_{j=1}^{N} \exp(i\bar{k}\underline{\underline{H}}(s_j)\Delta s_j) \qquad (10)$$

where $s_j = a + (j-1/2)\Delta s_j$, $\Delta s_j = (x-a)/N$, a denotes the transition region boundary, $\underline{\underline{H}}$ is the appropriate first-order Helmholtz equation matrix operator [2,4], and with the product of exponential factors ordered from right (lower j) to left (higher j) reflecting the noncommutativity of the matrix operator $\underline{\underline{H}}$ at different x. While product integration-based path integral constructions have been applied to the problems of nonrelativistic electron spin and the Dirac equation, such infinite products of matrices are, generally, only tractable in simple limiting cases [4,8].

Rather than starting from a transversely inhomogeneous formulation and, subsequently, building in backscatter effects, the generalization of Fourier methods to arbitrary inhomogeneous environments and the construction of a dynamical basis for the Helmholtz equation can proceed, in the second approach, from the construction of truly global configuration space path integrals, which attempt to generalize, for example, the homogeneous half-space result [3,7]

$$G^+(x,\underline{x}_t|0,\underline{x}_t') = \lim_{N\to\infty} \int_{R^{(n-1)(N-1)}} \prod_{j=1}^{N-1} d\underline{x}_{jt}\ (i\pi x N^{(n-1)N/2}$$

$$\cdot(\bar{k}K_0/2\pi\delta_{(n-1)N+1})^{((n-1)N+1)/2}\ H^{(1)}_{((n-1)N+1)/2}(\bar{k}K_0\delta_{(n-1)N+1})) \qquad (11)$$

where

$$\delta_{(n-1)N+1} = (N \sum_{j=1}^{N} (\underline{x}_{jt} - \underline{x}_{j-1t})^2 + x^2)^{1/2} \tag{12}$$

and $H_{\nu}^{(1)}(\xi)$ is the Hankel function. These elliptic-based (two-way) constructions, originating from the Fourier transform relationship between the Helmholtz and Schrödinger (parabolic) propagators, result in the approximate Feynman/Garrod path integral [3,7]

$$G(\underline{x}|\underline{x}') \simeq (-1/2\bar{k}^2) \lim_{N\longrightarrow\infty} \int_{R^{n(2N-1)}} \prod_{j=1}^{N-1} d\underline{x}_j \prod_{j=1}^{N} (\bar{k}/2\pi)^n d\underline{p}_j \frac{\exp(i\bar{k}S_N)}{(1/2 - \Sigma)} \tag{13}$$

where

$$S_N = \sum_{j=1}^{N} \underline{p}_j \cdot (\underline{x}_j - \underline{x}_{j-1}) \tag{14}$$

corresponds to an appropriate discretized action and

$$\Sigma = (1/N) \sum_{j=1}^{N} (p_j^2/2 + V(\underline{x}_j)) \tag{15}$$

plays a role analogous to an average energy with the identification $V(\underline{x}) = (-1/2)(K^2(x) - 1)$. For a transversely inhomogeneous half-space, partial integration of Eq.(13) in conjunction with the reflection principle (or method of images) results in [3,7]

$$G^{+}(x,\underline{x}_t|0,\underline{x}_t') \simeq \lim_{N\longrightarrow\infty} \int_{R^{(n-1)(2N-1)}} \prod_{j=1}^{N-1} d\underline{x}_{jt} \prod_{j=1}^{N} (\bar{k}/2\pi)^{n-1} d\underline{p}_{jt}$$

$$\cdot \exp(i\bar{k}(S_N + 2^{1/2}x(1/2 - \Sigma)^{1/2})) \tag{16}$$

with S_N and Σ taking on their appropriate forms in one-lower dimension.

Formally reducing both the full- and transversely inhomogeneous half-space phase space Feynman/Garrod path integrals to configuration space path integrals [7] establishes the path functional character of the representation. Moreover, the approximate Feynman/Garrod path integral is exact in the homogeneous medium limit, incorporates significant backscatter information, and contains both the geometrical (ray) acoustic and ordinary parabolic approximations. This configuration space formulation for the two-way problem, initially based on a variational principle and phase space constructions, seeks to express the propagator in terms of a phase

functional evaluated over an appropriate path space, as symbolically expressed in the Feynman/DeWitt-Morette representation [3,7,9]. This takes the form

$$G(\underline{x}|\underline{x}') = (-1/2\bar{k}^2) \int_E D(\underline{\zeta}) \exp(i\bar{k}\bar{W}(\underline{\zeta})) \tag{17}$$

where

$$\bar{W} = \int_{\underline{x}'}^{\underline{x}} \|d\underline{\zeta}\| \ (1 - 2V(\underline{\zeta}))^{1/2} \tag{18}$$

is the analog of the action associated with a "free particle" on a space with the metric

$$d\underline{l}^2 = (1 - 2V(\underline{\zeta}))\| d\underline{\zeta}\|^2 \tag{19}$$

and where E represents the space of paths from $\underline{x}'$ to $\underline{x}$ such that

$$1/2 = (1/\tau)\int_0^{\tau} dt \ ((1/2)\| d\underline{\zeta}(t)/dt\|^2 + V(\underline{\zeta}(t))) \tag{20}$$

with the constraints

$$\underline{\zeta}(0) = \underline{x}' \ ,$$

$$\underline{\zeta}(\tau) = \underline{x} \ . \tag{21}$$

The dynamical basis of the Helmholtz equation can, thus, be viewed in terms of a stochastic process embodying fixed "average energy" paths, or, alternatively, in terms of "free particle" motion [3,7,9].

III. COMPUTATIONAL ALGORITHMS. Direct integration of the one-way phase space path integral provides the computational basis for the pseudo-differential wave equation (2). Choosing the standard ordering, $F(\underline{u},\underline{v}) = \exp(-i\bar{k}\underline{u}\cdot\underline{v}/2)$, in Eqs. (6), (7), and (8) results in a numerically more efficient post-point marching algorithm in the form

$$\phi^+(x+\Delta x,\underline{x}_t) \simeq \int_{R^{n-1}} d\underline{p}_t \exp(i\bar{k}\underline{p}_t\cdot\underline{x}_t) \ (\exp(i\bar{k}\Delta x h_B(\underline{p}_t,\underline{x}_t))\hat{\phi}^+(x,\underline{p}_t)) \tag{22}$$

where $\hat{\phi}^+$ is the Fourier-transformed wave field and

$$h_B(\underline{p}_t,\underline{x}_t) = (k/\pi)^{n-1} \int_{R^{2n-2}} d\underline{s}dt \ \Omega_B(\underline{s},t) \exp(-2i\bar{k}(\underline{x}_t - t)\cdot(\underline{p}_t - \underline{s})). \tag{23}$$

This marching algorithm provides the generalization of the Tappert/Hardin split-step FFT algorithm [1] to the full one-way (factored Helmholtz) wave equation. For a two-dimensional model ocean/bottom propagation environment with a perfectly reflecting ocean surface, the Fourier transform of the wave field in Eq.(22) is replaced by a discrete fast sine transform and the inverse transform is evaluated by a rectangular rule integration, enabling the propagated wave field to be expressed in the matrix form

$$\phi^{+}(x+\Delta x, z_n) = \sum_m A_{nm} \hat{\phi}^{+}(x, p_m) \tag{24}$$

for each depth point z_n. In Eq.(24), ϕ^+ and $\hat{\phi}^+$ are column vectors and the matrix $\underline{\underline{A}}$ is defined by its matrix elements

$$A_{nm} = \eta \sin(\bar{k} p_m z_n + \bar{k}\Delta x h_B^o(p_m, z_n)) \exp(i\bar{k}\Delta x h_B^e(p_m, z_n)) \tag{25}$$

where h_B^e and h_B^o are the even and odd parts with respect to p of $h_B(p,z)$ in Eq.(23) and η is an appropriate transform normalization constant [1,4,12].

The principal idea underlying the practical implementation of the phase space marching algorithm is the construction of a small number of approximate operator symbols, which, when taken together, allow for wave field computations over a very wide range of model environments and propagation parameters. In conjunction with a study of exactly soluble cases of the Weyl composition equation [6], high-frequency, real Weyl high-frequency, uniform high-frequency, and low-frequency approximate symbols have been constructed [2-4,6]. Of particular significance is the fact that the manner of marching the radiation field is independent of the medium and any approximation to the square root Helmholtz operator, resulting in a modular code architecture and highly versatile propagation program. Moreover, the propagation models constructed and computed through the code correspond to singular integro-differential equation as well as partial differential equation approximations to the one-way wave equation. Indeed, this numerical algorithm represents one of the very few attempts to compute directly with pseudo-differential and Fourier integral operators. For the two-dimensional case, the range-incrementing procedure is just a sequence of matrix multiplications, and, thus, ideally suited for computers which provide either a vector or a parallel pipe type of operation. Phase space filtering reduces both the size of the matrix multiplication and the number of matrix elements initially computed, in particular, reducing the total range-incrementing computational time by almost an order of magnitude for typical model calculations [4].

Numerical results of transmission loss (dB re 1 m) as a function of range (km) for a number of model ocean/bottom propagation experiments demonstrate the computational viability of the factorization-/path integration-based phase space marching algorithm [4,12]. Several propagation experiments are summarized in Figures 3, 5, and 7, with the corresponding transmission loss curves compared with a reference Fast Field Program (FFP) algorithm [4,12] in Figures 4, 6, and 8.

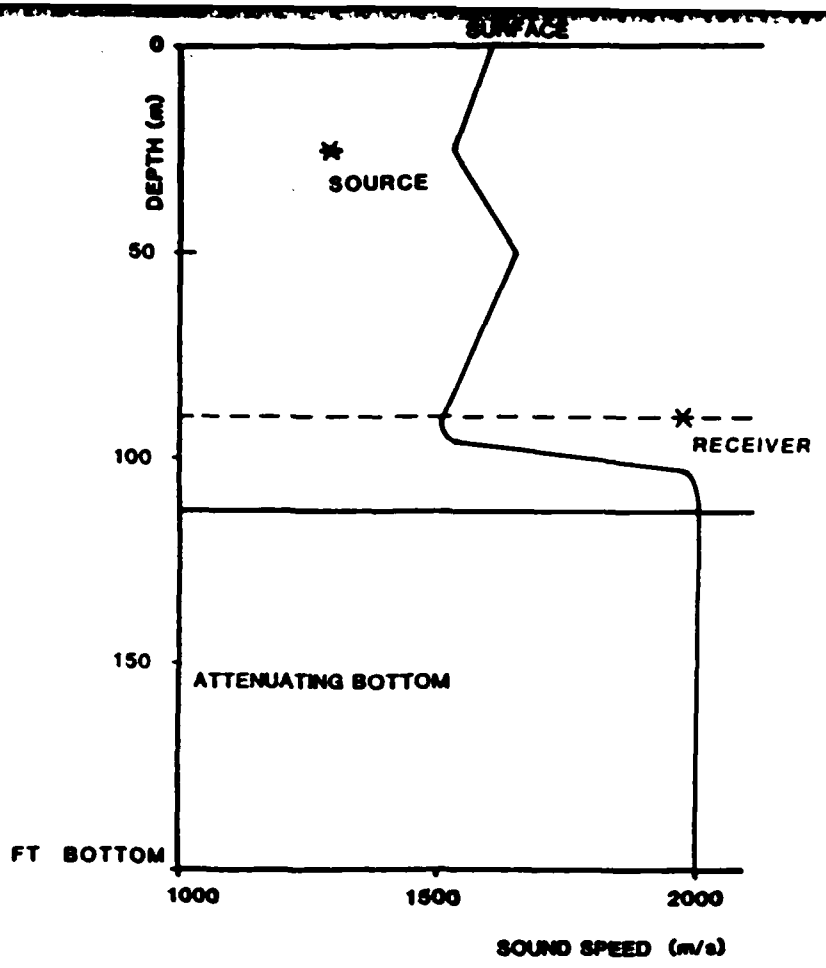

Fig. 3. Model environment 1 and propagation experiment.

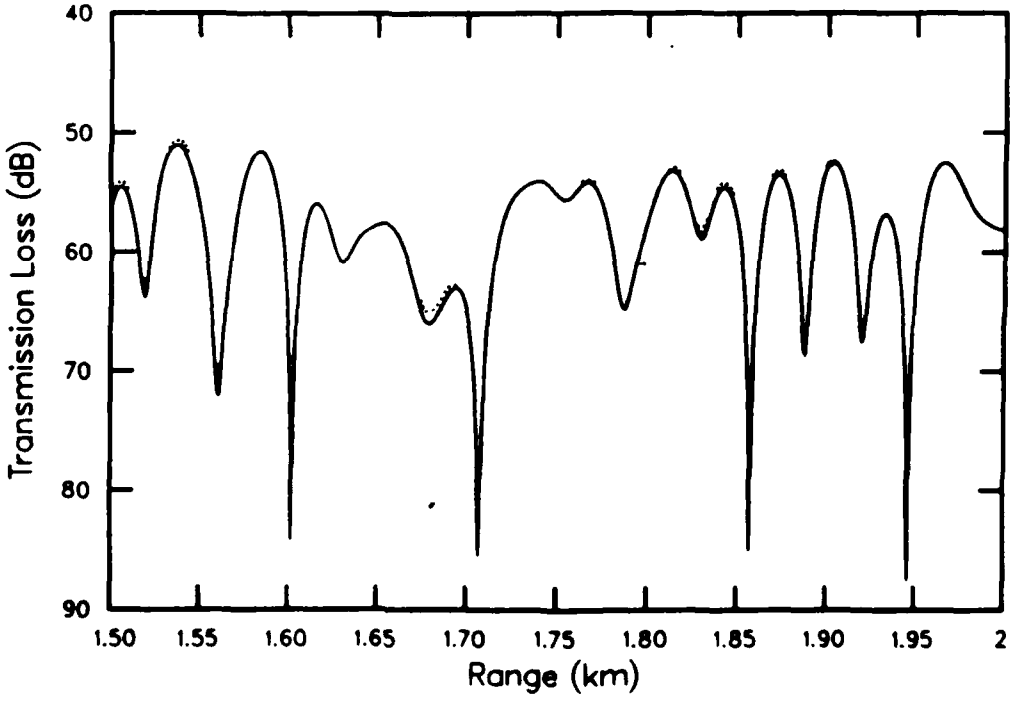

Fig. 4. Transmission loss (dB re 1 m) versus range (km) for model environment 1 at 400 Hz. (——) High Frequency (80 degree filter) (....) FFP

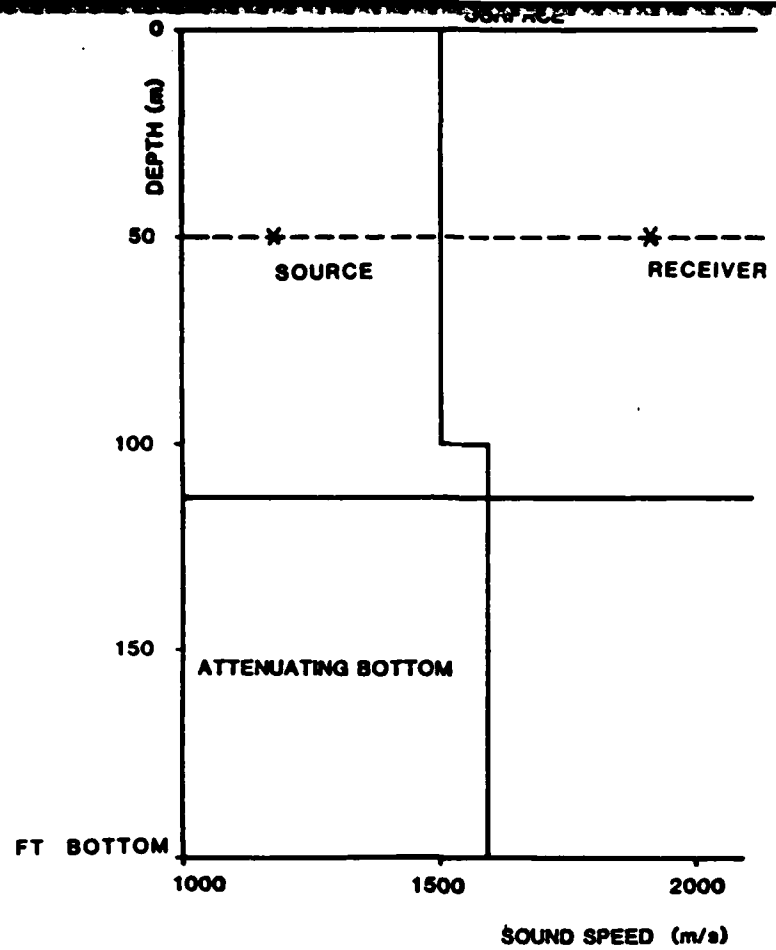

Fig. 5. Model environment 2 and propagation experiment.

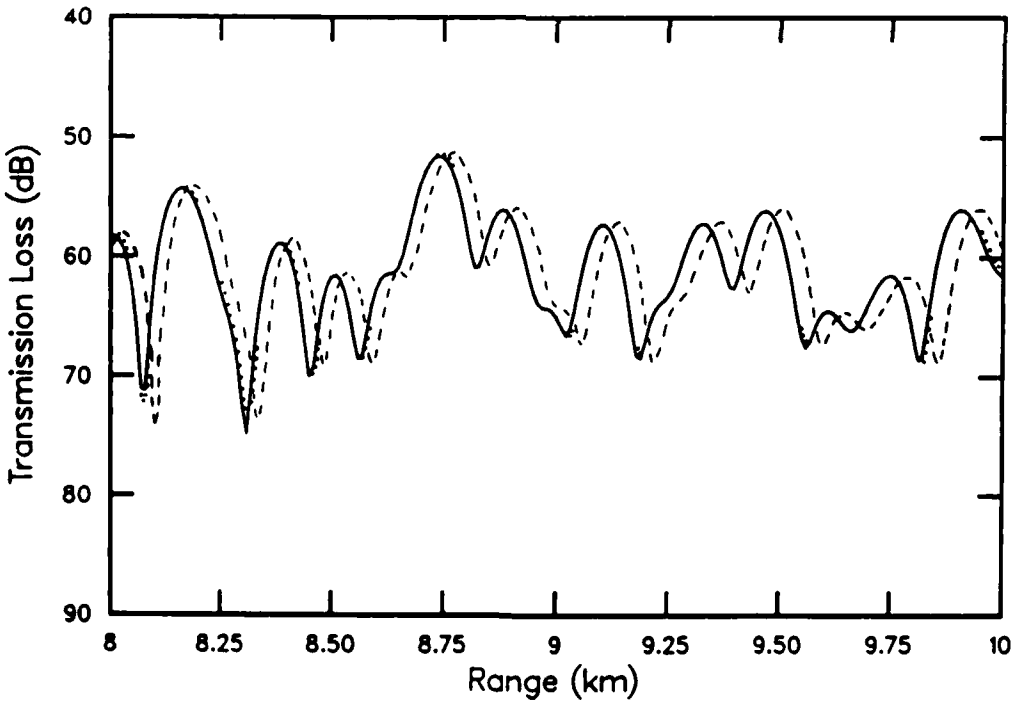

Fig. 6. Transmission loss (dB re 1 m) versus range (km) for model environment 2 at 250 Hz. (——) High Frequency (60 degree filter) (----) High Frequency (....) FFP

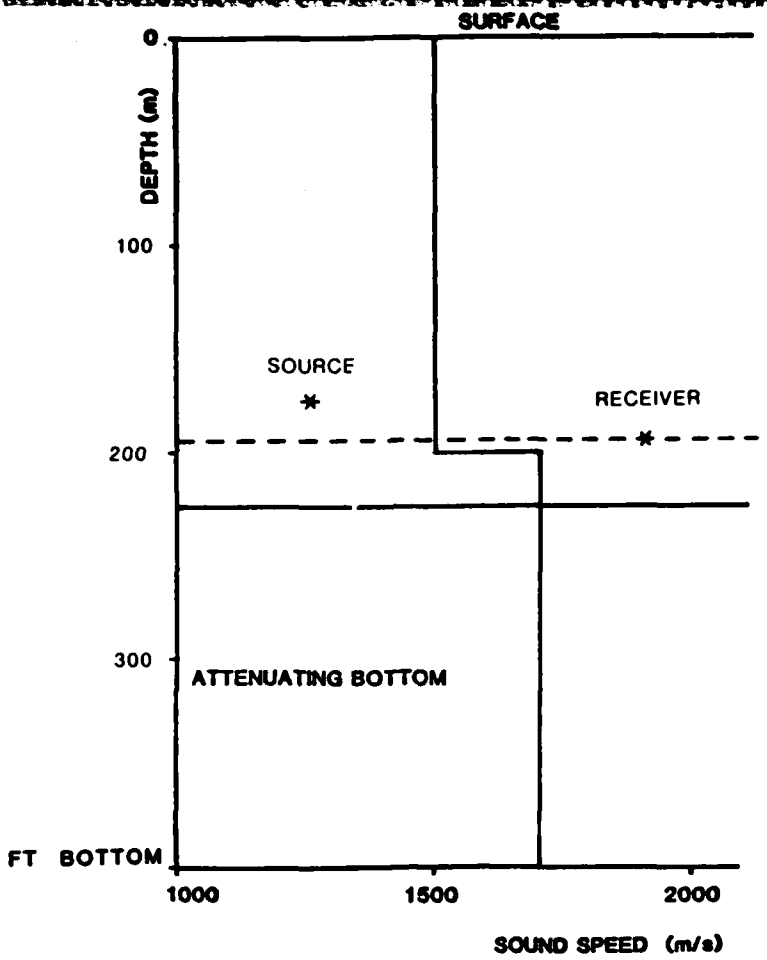

Fig. 7. Model environment 3 and propagation experiment.

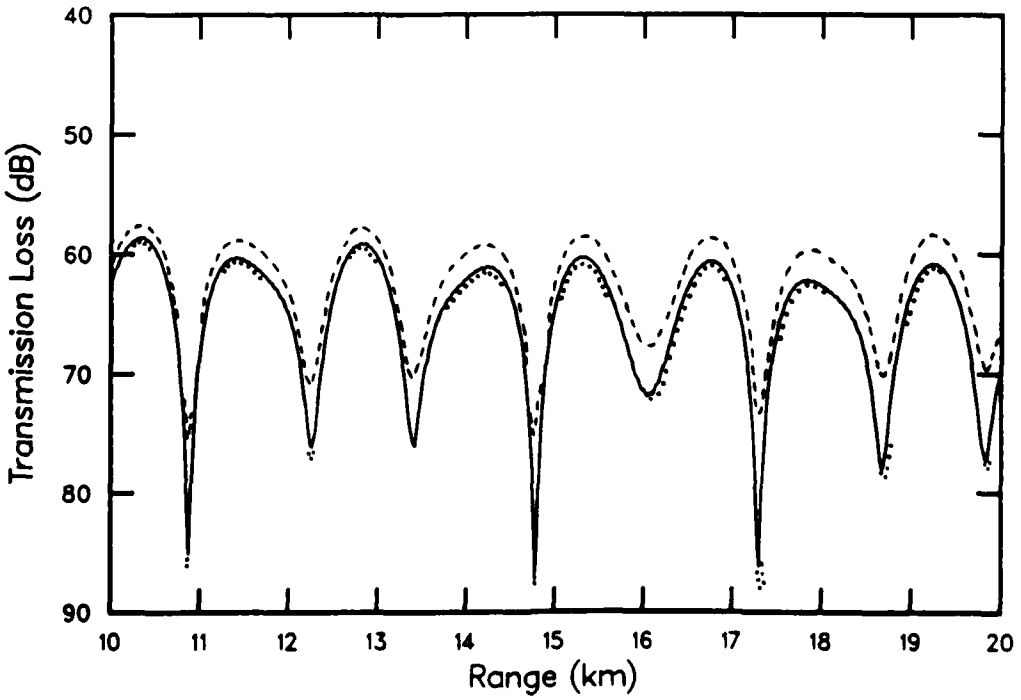

Fig. 8. Transmission loss (dB re 1 m) versus range (km) for model environment 3 at 25 Hz. (——) Real Weyl High Frequency (----) High Frequency (....) FFP

For 400 Hz propagation in the exaggerated double-well model of Figure 3, a wide-angle capability well beyond the ordinary parabolic approximation is required. Figure 4 illustrates the excellent agreement between the high-frequency and FFP algorithms over ranges on the order of 500 wavelengths. Figure 6 illustrates the cumulative growth of a phase shift error at long range which characterizes the breakdown of the high-frequency algorithm in the 250 Hz propagation in the rapidly changing shallow-water model of Figure 5. Combining Fourier component, or wave number, filtering with the high-frequency algorithm leads, not only to a more efficient and, thus, faster algorithm, but also, to a more widely applicable numerical scheme. The filtering, in addition to removing Fourier components which, in principle, make no significant contribution to the computed wave field, eliminates those unnecessary regions of phase space where the small error in the high-frequency symbol approximation can lead, in a cumulative manner, to serious discrepancies at sufficiently long ranges. This is particularly well illustrated in the 60 degree filtered calculation on model environment 2 at 250 Hz which results in the complete elimination of the cumulative phase shift error (Figure 6), greatly extending the effective computational range. Sufficiently decreasing the propagation frequency and increasing the jump discontinuity in the sound speed, as illustrated in the 25 Hz propagation in the shallow-water model of Figure 7, demonstrate the violation of energy conservation inherent in the high-frequency wave theory and the now-rapid decay with increasing range of the corresponding numerical algorithm. This growth in the wave field, illustrated in Figure 8, is eliminated by the real Weyl high-frequency algorithm [4], which effectively restores energy conservation, as is also illustrated in Figure 8. A more detailed discussion of these and other points is presented elsewhere [1,4,12].

The speed and modest storage requirements of the filtered one-way algorithm indicate that range-dependent calculations over extended environments should be feasible with current supercomputer technology. Both range-updating and the numerical calculation of the reflected and transmitted fields from an interface should be possible over distances on the order of 10^4 wavelengths. Preliminary computations with range-dependent Munk-profile deep ocean environments, including propagation through extended shadow regions, compare well with adiabatic normal-mode calculations.

Both the range-dependent and range-independent Feynman/Garrod path integral representations can be computed by standard Monte Carlo (statistical sampling) methods for the numerical evaluation of multiple integrals [4]. While numerically calculating Helmholtz wave fields as high (in principle, infinite)-dimensional integrals is quite distinct from the more traditional finite-difference and finite-element approaches, the Monte Carlo evaluation of functional integrals has been successfully applied in quantum mechanical, statistical mechanical, and quantum field theoretical calculations [4]. For the phase space representations of Eqs. (13) and (16) in two dimensions ($n = 2$), the modeling of realistic propagation experiments can involve the computation of thousand-dimensional oscillatory integrals. Correlated-sampling variance reduction techniques can dramatically improve the speed and accuracy of the algorithm [4]. Generally speaking, a large parallel processing capability should have a very favorable impact on the numerical computation of path integrals [4].

IV. INVERSE FORMULATION. The phase space-based construction of the

square root Helmholtz operator provides the basis for a formulation of the inverse algorithms mentioned in the Introduction. Mathematically, the refractive index field (or its square) is reconstructed from the full-space Helmholtz Green's function G through the relationship

$$B(\underline{x}_t,\underline{x}'_t) = (2i/k) \lim_{x \longrightarrow 0} (\partial_x^2 G(x,\underline{x}_t|0,\underline{x}'_t)). \tag{26}$$

The symbol $\Omega_B(\underline{p},\underline{q})$ is then constructed through an inverse Fourier transform of the kernel function $B(\underline{x}_t,\underline{x}'_t)$ and subsequently yields the refractive index field upon a direct application of the Weyl composition equation (3) for $|\underline{p}| = 0$. In the homogeneous medium limit, the direct evaluation of the composite symbol reduces to the square of the symbol, $\Omega_B 2(\underline{p},\underline{q}) = \Omega_B^2(\underline{p},\underline{q})$.

The inverse algorithm proceeds around the correspondence diagram (pictorial summary) in a counterclockwise fashion. The direct propagation algorithm requires the inversion of Eq.(3) while the inverse propagation algorithm only requires a direct computation of Eq.(3). Thus the direct propagation problem has been transformed into an "inverse" problem while the wave field inversion problem has been reformulated, in an appropriate sense, as a direct calculation.

The factorization algorithm exactly inverts the inherently nonlinear relationship between the wave field data and the refractive index field as reflected in the Lippmann-Schwinger equation for the propagator [3]. Most importantly, it is a multidimensional formulation. For the "physical experiment," a point source is introduced into the medium defining the initial-value ($x = 0$) plane. The second derivative with respect to the range of the wave field is then determined as a function of the point source and receiver positions. Collecting the data on the initial-value plane would most probably limit the application of the algorithm to specific types of bore-hole experiments. Moreover, mathematically, the inversion requires the evaluation of singular integrals (generalized functions). Collecting data on a downfield plane ($x > 0$) leads to a transmission experiment similar to the oceanic sound speed profile inversion method of DeSanto [3]. The downfield wave field provides for an appropriate analytic continuation in the factorization algorithm and connects the analysis with the inverse diffraction problem [3].

The transmission, or propagation, formulation is analogous to tomography. The reference wave number in the factorization analysis corresponds to $2\pi/$(Planck's constant) as opposed to its square playing the role of an energy. The source generation and data collection over parallel planes then naturally correspond to the multidirectional insonifying plane waves and subsequent angular data collection of fixed-energy (frequency) diffraction tomography [3]. For range-dependent environments, the inclusion of backscatter effects, even in an approximate manner, would then provide the basis for a generalized acoustic tomography, extending the diffraction algorithms based on the Born, Rytov, or distorted-wave Born approximations [3]. The nonlinear factorization and subsequent weak-backscatter perturbation theory would extend the linearized weak-scattering treatments into the nonlinear regime. This can be attempted in two ways. Formal field splitting analysis provides the basis for a weak-backscatter perturbation theory within the framework of invariant imbedding [2-4]. The arbitrary-

dimensional nature of the factorization analysis in conjunction with mathematical imbedding concepts provides the basis for a spatial-dimensional perturbation theory [2-4]. This essentially involves treating the spatial dimension of both the Helmholtz operator, in general, and the refractive index field, in particular, as a variable and subsequently studying the structure of the resulting family of systems indexed in this manner. For the case of two (different) transversely inhomogeneous half-spaces separated by a planar interface, an inverse algorithm can be initially based on the composition equation (9).

For a transversely inhomogeneous environment, the factorization inversion model invites comparison with "effective one-dimensional" stratified environmental models such as that of Stickler and Deift [4]. In both models, the location of the field source (finite) and the data measurements is within the scattering region. Most importantly, the factorization method is a direct inversion of an arbitrary-dimensional propagation equation which requires less symmetry than those models (i.e., Stickler-Deift) reducible to the standard one-dimensional formulation of Deift-Trubowitz [4] or Gelfand-Levitan [4]. Thus for example, in a general n-dimensional Cartesian formulation, the refractive index field can be a function of as many as (n-1) coordinates in the factorization model, while a function of only one coordinate in an "effective one-dimensional" model. The experiment envisioned and the distinguished direction differ in the two models. In the transversely inhomogeneous environment, the direction in which there is medium homogeneity is distinguished, while in the "effective one-dimensional" model, the one direction in which there is medium inhomogeneity is, in effect, distinguished. Data, in both cases, is collected perpendicular to the distinguished direction. The Stickler-Deift model is essentially a one-dimensional scattering experiment with the surface data, in effect, reflection coefficient data. Thus unlike the transmission experiment, which extensively samples the region of inhomogeneity, in the factorization model, the Stickler-Deift analysis does not account for the presence of "trapped modes" [4]. The formal inclusion of a specific pressure-release surface within the pseudo-differential operator framework would allow for a stratified environmental model and the subsequent quantitative comparison with the Stickler-Deift model.

For applied inverse problems, approximate inversions may prove adequate. Approximate inversion algorithms follow readily from the perturbative treatments of the Weyl composition equation. $K^2(\underline{q})$ is related to $\Omega_B(0,\underline{q})$ in a quadratic fashion and through a linear integral relationship, respectively, in the high-frequency ($\bar{k}\longrightarrow\infty$) and weak-inhomogeneity (Born) limits. In particular, the high-frequency algorithm is based upon choosing, in practice, a $|\underline{p}|$ such that the symbol approaches its asymptotic form, $\Omega_B(\underline{p},\underline{q}) \sim (K^2(\underline{q}) - \underline{p}^2)^{1/2}$. The approach to the asymptotic regime in phase space is governed both by the magnitude of $K^2(\underline{q}) - \underline{p}^2$ (large) and the variation of the refractive index field on the wavelength scale (small). Figure 9 illustrates the high-frequency inversion for the case of a quadratic medium. Applying the full composition equation for the inversion would result in a linear function in X for the real part and an imaginary part which is identically zero. Finally, weighted Hilbert space methods for incorporating prior estimates appear to be applicable to the Fourier-based factorization approach [4].

ACKNOWLEDGMENTS

This work was supported under grants from the Office of Naval Research (N00014-85-K-0307) and the U.S. Army Research Office (DAAG 29-85-K-0002).

REFERENCES

1. J.A. Davis, D. White, and R.C. Cavanagh, "NORDA Parabolic Equation Workshop," NORDA tech. note 143, Naval Ocean Research and Development Activity, NSTL Station (1982).
2. L. Fishman and J.J. McCoy, Derivation and application of extended parabolic wave theories. Part I. The factorized Helmholtz equation, J. Math. Phys., 25 (2): 285 (1984).
3. L. Fishman and J.J. McCoy, Factorization, path integral representations, and the construction of direct and inverse wave propagation theories, IEEE Trans. Geosc. Rem. Sens., GE-22 (6): 682 (1984).
4. L. Fishman, J.J. McCoy, and S.C. Wales, Factorization and path integration of the Helmholtz equation: numerical algorithms, J. Acoust. Soc. Am., submitted for publication (1986).
5. M.E. Taylor, "Pseudodifferential Operators," Princeton University Press, Princeton (1981).

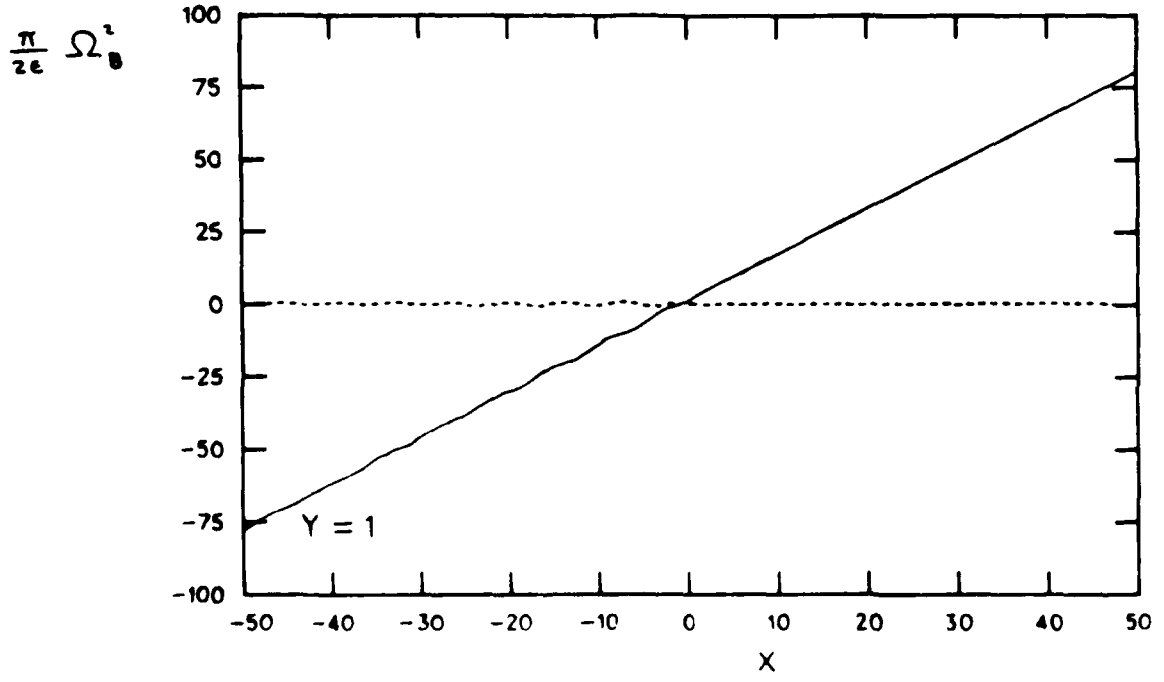

Fig. 9. The real (——) and imaginary (----) parts in the high-frequency approximate inversion for the n = 2 quadratic medium.

6. L. Fishman and A. Whitman, Exact and uniform perturbation solutions of the Helmholtz composition equation, J. Math. Phys., submitted for publication (1986).
7. L. Fishman and J.J. McCoy, Derivation and application of extended parabolic wave theories. Part II. Path integral representations, J. Math. Phys., 25 (2): 297 (1984).
8. L.S. Schulman, "Techniques and Applications of Path Integration," Wiley, New York (1981).
9. C. DeWitt-Morette, A. Maheshwari, and B. Nelson, Path integration in nonrelativistic quantum mechanics, Phys. Rep., 50 (5): March (1979).
10. J.J. McCoy, L. Fishman, and L.N. Frazer, Reflection and transmission at an interface separating transversely inhomogeneous acoustic half-spaces, Geophys. J. R. Astr. Soc., to appear (1986).
11. J.J. McCoy and L.N. Frazer, Propagation modelling based on wave field factorization and invariant imbedding, Geophys. J. R. Astr. Soc., to appear (1986).
12. L. Fishman and J.J. McCoy, A new class of propagation models based on a factorization of the Helmholtz equation, Geophys. J. R. Astr. Soc., 80: 439 (1985).

PUBLICATIONS DURING PERIOD OF FUNDING

L. Fishman, "Phase Space Methods and Path Integration: the Analysis and Computation of Scalar Wave Equations," in Proceedings of the International Congress on Computational and Applied Mathematics, J. Comp. Appl. Math., to appear (1987).

L. Fishman and S.C. Wales, "A Fast, Filtered, Fourier-Transform Marching Algorithm for Wide-Angle, One-Way Wave Propagation," in Proceedings of the 1st IMACS Symposium on Computational Acoustics, edited by D. Lee, R.L. Sternberg, M.H. Schultz, and R. Vichnevetsky (North Holland, Amsterdam, 1987).

L. Fishman, "Phase Space Methods and Path Integration: the Construction of Numerical Algorithms for Computational Acoustics," in Underwater Acoustics, edited by H. Merklinger (Plenum Press, New York, 1987).

L. Fishman "Phase Space Methods and Path Integration: a Miscroscopic Approach to Direct and Inverse Wave Propagation," in Proceedings of the Fourth Army Conference on Applied Mathematics and Computing, edited by J. Chandra (U.S. Army Research Office, Research Triangle Park, 1987).

L. Fishman and A. Whitman, "Exact and Uniform Perturbation Solutions of the Helmholtz Composition Equation," J. Math. Phys., submitted for publication (1986).

L. Fishman, J.J. McCoy, and S.C. Wales, "Factorization and Path Integration of the Helmholtz Equation: Numerical Algorithms," J. Acoust. Soc. Am., submitted for publication (1986).

L. Fishman, "Path Integral-Based Numerical Algorithms for Computational Acoustics," in Proceedings of the 12th International Congress on Acoustics Sysposium on Underwater Acoustics, edited by H. Merklinger (12th ICA, Toronto, 1986).

L. Fishman, J.J. McCoy, and S.C. Wales,"Factorization and Path Integration of the Helmholtz Equation: Numerical Algorithms," in IMACS Transactions, Vol. 1-Numerical Analysis and Applications, edited by R. Vichnevetsky and J. Vignes (North Holland, Amsterdam, 1986).

J.J. McCoy, L. Fishman, and L.N. Frazer, "Reflection and Transmission at an Interface Separting Transversely Inhomogeneous Acoustic Half-Spaces," Geophys. J. Roy. Astro. Soc. 85, 543 (1986).

L. Fishman and S.C. Wales, "Factorization and Path Integration of the Helmholtz Equation: Numerical Algorithms," in Ocean Seismo-Acoustics, edited by T. Akal and J.M. Berkson (Plenum Publishing Corporation, New York, 1986).

J.J. McCoy, L. Fishman, L.N. Frazer, "Range Dependent Propagation Coded Based on Wave Field Factorization and Invariant Imbedding," in Ocean Seismo-Acoustics, edited by T. Akal and J.M. Berkson (Plenum Publishing Corporation, New York, 1986.

L. Fishman, J.J. McCoy, and S.C. Wales, "Factorization and Path Integration of the Helmhotz Equation: Numerical Algorithms." in Proceeding Volume 2: 11th IMACS World Congress on System Simulation and Scienfific Somputation, edited by B. Wahlstrom, R. Henriksen, and N. P. Sundby (NFA, Oslo, 1985), Page 139.

END

4-87

DTIC

END

4-87

DTIC